Microcrystal electron diffraction for the study of protein-ligand interactions and the potential for drug discovery

Lisa Clark, Guanhong Bu, Brent L. Nannenga* and Tamir Gonen*

Department of Biological Chemistry, University of California, Los Angeles, CA, USA

Lisa Clark and Tamir Gonen

Chemical Engineering, School for Engineering of Matter, Transport and Energy, Arizona State University, Tempe, AZ USA

Guanhong Bu and Brent L. Nannenga

Center for Applied Structural Discovery, Biodesign Institute, Arizona State University, Tempe, AZ, USA

Guanhong Bu and Brent L. Nannenga

Department of Physiology, University of California, Los Angeles, CA, USA

Tamir Gonen

Howard Hughes Medical Institute, University of California, Los Angeles, CA, USA

Tamir Gonen

*email: brent.nannenga@asu.edu and tgonen@g.ucla.edu

Abstract | Microcrystal electron diffraction (MicroED) is an electron cryo-microscopy (cryo-EM) technique used to determine molecular structures with crystals that are a millionth the size needed for traditional single crystal X-ray crystallography. An exciting use of MicroED is in drug discovery and development where it can be applied to the study of proteins and small molecule interactions and for structure determination of natural products. In this Perspective we discuss the current applications of MicroED for structure determination of protein-ligand complexes and potential future applications in drug discovery.

Introduction

Understanding the interactions between small molecules and their protein targets is critical for fundamental studies of ligand binding, and drug development and optimization. The most common method used to study high-resolution structural details of ligand-protein and drug-protein complexes is X-ray crystallography [1-3]. However, structure determination by X-ray crystallography can be hindered by the requirement of large crystals, which can be difficult to produce. Moreover, natural products are often isolated from native sources in very small amounts that are insufficient for large crystal growth. Therefore, there is a need for the development of structure determination methods for data collection using less material and, therefore, smaller crystals [4-8]. Electrons are able to produce diffraction data from significantly smaller crystals than those required for X-rays [9,10] — electrons have a much stronger interaction with matter, and a reduction in damage per elastic scattering event. Therefore, methods that use electrons rather than X-rays can employ crystalline samples previously considered much too small for structural analysis by conventional approaches. In addition to the development of electron-based approaches, cryogenic embedding, which can preserve the samples and limit radiation damage, has also emerged. The cryo-electron microscopy (EM) method microcrystal electron diffraction (MicroED) uses a transmission electron microscope (cryo-TEM) to collect electron diffraction data, extremely low exposures for atomic structure determination, and vanishingly small crystals that are sometimes seemingly amorphous [8,11,12]. The diffraction data are collected whilst the stage is continuously rotated, which produces data analogous to data collected by single crystal X-ray diffraction. Thereby, the data can be processed using commonly used programs developed for X-ray crystallography. Other electron crystallography methods have also been developed, which can study radiation hardy materials, inorganic salts and metal organic frameworks at room temperature (for example, Automated diffraction tomography (ADT), Rotation electron diffraction (RED)) [13-22]; however, these methods are currently not used for macromolecular protein structure determination. MicroED was specifically developed for the study of macromolecular protein structure as an extension of electron crystallography of 2D crystals in the field of cryo-EM. It has successfully been used to determine structures from a wide variety of samples including globular protein macromolecules [23-27], membrane proteins [28-31] and peptides [32-36], and it is also useful to study small organic molecules, natural products [12,37-43], and materials [44-48]. While other cryo-EM modalities, such as single particle analyses, show promise for drug discovery [49-51], in this Perspective we focus on the use of MicroED for determining the structures of protein-ligand complexes, which will provide the background and perspective on the application of MicroED within the field of drug discovery [52,53].

MicroED methodology

Detailed procedures for MicroED have been described previously [54-57]. Here, we summarize the general MicroED process for the study of biomolecular samples. The workflow for MicroED experiments begins with applying the sample to the surface of a carbon-coated EM grid, and blotting away excess crystallization solution. Following the removal of excess solution, the grid is plunged into liquid ethane for vitrification. Blotting and vitrification are generally performed using standard automated or manual plunge-freeze devices that are commonly used across cryo-EM laboratories [58]. Recently, new MicroED specific sample preparation techniques have been developed [59], and new methods are expected to continue to enhance sample preparation. Following vitrification, the samples can be analyzed by cryo-EM immediately or stored long-term in liquid nitrogen.

MicroED is performed at liquid nitrogen temperatures using a cryo-EM that is equipped with a high-speed scintillation-based camera, hybrid-pixel detector, or direct electron detector [37,60-64]. We make a note that we have not used hybrid-pixel detectors in our respective laboratories, so we cannot comment on the ease of use but have included these for reference. Depending on the type of cryo-EM used, samples are either loaded onto a side entry cryo-holder or are placed into a cartridge for loading into a cryo-EM equipped with an autoloader. Once in the microscope, the samples are imaged at low magnification to locate regions of the grid with appropriate sample thickness and microcrystal density. This can be done manually, or with the help of automation software [65,66]. Areas of interest are then investigated by imaging at a very low electron dosage and higher magnification such that a single grid square occupies the field of view. At this point, crystals are located and preliminary diffraction patterns are collected to determine the quality of each individual microcrystal. MicroED data sets can then be collected from the crystals which show high-quality diffraction (for example, sharp well-separated reflections to high-resolution). MicroED data are collected by continuous rotation of the cryo-TEM stage with concurrent high-speed detector recordings [24]. Recent work with high-speed data collection using sensitive detectors has demonstrated that MicroED data sets can be collected at extremely low doses (less than 1 e^{-} $Å^{-2}$ total dose), which greatly limits the exposure of the sample to the electron beam and therefore limits radiation damage [61,67,68]. At these ultra-low doses, MicroED data sets can be indexed, integrated, and merged through the use of standard crystallographic programs such as MOSFLM, DIALS and XDS [69-72]. Depending on the diffraction quality, crystal orientation, and crystal symmetry, several data sets can often be merged together to increase crystallographic completeness for structure solution and refinement. These data sets are then used for structure

determination and the resulting models and maps can be used for detailed structural analysis of the sample.

Protein-ligand complexes

Protein-ligand complexes are important structures to study for drug discovery, and difficult to study crystals of these complexes can be studied by MicroED. One of the early proteins examined with MicroED was catalase from bovine liver [23]. In this instance, a single microcrystal that was approximately 150 nm thick was used to determine the structure of catalase to 3.2 Å resolution. The homotetrameric structure of catalase contains a bound heme in each one of its four monomers, and this was used as an initial test for the ability of MicroED data to determine the presence of ligands in the resulting structure. When the experimental maps were calculated with a model lacking the heme ligands, there was significant positive density demonstrating that bound ligands could be located by MicroED when they are not initially included in the atomic models (Fig. 1a). A similar test was performed with these data on the catalase-bound NADPH, where one NADPH molecule is tightly bound to each catalase monomer. As with the heme tests, maps were calculated using a previously determined model lacking NADPH [23]. These maps showed positive differences for both the location of the NADPH as well as the NADPH-bound conformation of residue F197 (Fig. 1b), which indicates that MicroED data are of sufficient quality to identify subtle conformational differences due to ligand binding. In another study on catalase, the sensitivity of electron diffraction to the effects of charge was demonstrated on the residues which interact with the bound heme ligand [31], which highlights the potential of this technique on the study of how charge influences ligand binding.

While the initial work on catalase was an important demonstration of the ability to identify ligands, the heme and NADPH molecules are already part of the native structure of catalase. An improved method for the incorporation of new ligands into microcrystals was recently reported using the enzyme proteinase K soaked with 5-amino-2,4,6-triodoisophthalic acid (I3C) [73]. In this approach, proteinase K microcrystals were applied to a carbon-coated EM grid and the excess liquid was blotted away, similar to standard MicroED sample preparation procedures. However, rather than immediately vitrifying the sample, additional crystallization solution containing the I3C ligand was added to the surface of the grid to incubate together with the crystals. Following incubation, the ligand solution was blotted from the grid and the sample was plunged into liquid ethane for vitrification. The structure that resulted from MicroED data collected using these on-grid soaked crystals showed strong positive denisty for four bound I3C ligands. When a similar experiment was performed with larger crystals for X-ray crystallography only three I3C molecules

were identified, and these sites had lower occupancy and therefore less defined maps relative to the MicroED maps (Fig. 2). This report suggests that soaking small microcrystals and using MicroED for data collection has the potential of improving the modeling of bound ligands in protein structures relative to soaking larger crystals.

Inhibitor-bound proteins

The drug bevirimat is an inhibitor of HIV maturation and acts on the HIV Gag capsid protein by binding to it and preventing protease cleavage [27]. The detailed interaction between bevirimat and Gag and how this may prevent protease activity was difficult to determine as soaking large HIV-1 Gag crystals with bevirimat reduced crystal quality and co-crystallization efforts were unsuccessful. However, by soaking nanocrystals of the C-terminal domain SP1 spacer peptide (CTD-SP1) HIV-1 Gag with bevirimat, crystal quality could be preserved, and MicroED could be used to produce a 2.9 Å resolution structure of bevirimat bound to HIV-1 Gag (Fig. 3a) [27]. This structure sheds light on how bevirimat can bind to HIV Gag and the potential strategies for further drug discovery to target this critical protein. Additionally, this study demonstrated how MicroED could be used to determine the structure of difficult drug-protein complexes and aid structure-based drug discovery.

In other work, MicroED has been used to determine the interaction of the sulfonamide inhibitor, acetazolamide (AZM), with human carbonic anhydrase (HCA II) [62]. Here, the AZM bound structure of HCA II was determined to 2.5 Å resolution, with sufficiently high-quality data to directly fit the entire molecule into the experimental maps, which enabled a clear visualization of the drug-protein interactions (Fig. 3b). Although the structure of AZM bound HCA II had been determined previously by X-ray crystallography [74], the MicroED structure of AZM-HCA II further demonstrated that MicroED can be used to model pharmaceutically relevant compounds bound to proteins at high-resolution.

Drug–membrane-protein interactions

Membrane proteins account for approximately 30% of all proteins, and carry out essential functions, such as signal transduction, energy conversion, and selective transport. Thereby, membrane proteins represent key drug targets. Membrane protein structure determination is notoriously difficult, and novel methods for the study of membrane protein structure and function are in high demand. Recently, MicroED has been applied to membrane protein structures, which opens the door to the study of membrane protein to molecule interactions. The potential for high-quality MicroED structures of membrane proteins was demonstrated by non-selective cation

channel NaK analysis [29]. NaK nanocrystals were used to produce a 2.5 Å structure (Fig. 4a), where two new conformations of the external Na^+ binding sites were determined.

While NaK crystals grow in a detergent solution, which makes them suitable for standard MicroED sample preparation methods, many important membrane proteins are crystallized in more viscous media, such as lipids, which make sample preparation very difficult. Therefore, new methods of preparing these samples are required. A powerful tool for handling thicker samples is the use of a cryo-focused ion beam (cryo-FIB), which allows the selected thinning of thicker samples down to approximately 200 nm [75-78]. These thinned layers are then transferred from the cryo-FIB to the cryo-EM and used for MicroED data collection. This cryo-FIB milling approach was critical to the recent 3.1 Å structure determination of a lipid embedded mammalian anion channel [28]. When the density maps are viewed for these data, additional unmodelled density was observed surrounding the channel, which indicates the presence of lipids around the proteins. Thereby, there is a potential for membrane protein bound molecules to be resolved even at moderate resolutions by MicroED.

G-protein coupled receptors (GPCRs) are an important class of receptors, which are typically crystallized in the viscous lipidic cubic phase (LCP). LCP is very difficult to work with and produces samples that are still too thick to be handled by cryo-FIB milling. Therefore, additional sample handling procedures were required to investigate samples grown in LCP with MicroED [79]. When improved handling procedures were combined with cryo-FIB milling, it was reported that a single GPCR microcrystal could be analyzed by MicroED to yield a high-resolution structure [30]. The structure of the human adenosine (A_{2A}) receptor was determined to 2.8 Å resolution (Fig. 4b), and several bound molecules were identified in the structure. Four cholesterol molecules could be placed within the difference maps and an antagonist (ZMA), which was present during crystallization, could be placed within the A_{2A} receptor ligand binding site (Fig. 4c). This demonstrates the use of MicroED to determine the structure of a GPCR from LCP along with the successful identification of bound ligands, which paves the way for future MicroED driven structural investigation of important GPCR-drug complexes.

Conclusion

While X-ray crystallography has been an important tool for drug discovery, MicroED has been a successful method for high-resolution structure determination from nano and microcrystalline material. By removing the need for larger crystal growth and, in some cases, improving the results of ligand soaking experiments through the use of smaller crystals, MicroED can increase the rate in which protein-ligand complexes can be studied. The main hurdles for MicroED so far have been

limited access to instrumentation and the ability to prepare high-quality samples for data collection. As more institutions invest in cryo-EM, additional instrumentation is slowly becoming available — although the majority of microscope time is typically allocated to other cryo-EM modalities, such as single particle cryo-EM and cryo-electron tomography, and not for MicroED. For this reason, dedicated instrumentation for MicroED is needed and nationally funded centers must be established to provide access to the technology. Moreover, through the development of automation for other structural biology techniques, in addition to higher throughput data collection methods for MicroED, and serial crystallography approaches, there is promise to further increase the ease and volume of MicroED experiments [65,66,80,81]. As with all cryo-EM methods, sample preparation remains a challenging step in the overall pipeline. Recent advancements in sample handling and preparation methods [59,73,79], including the application of cryo-FIB milling [75-78], promise to improve the success rate of MicroED experiments. However, continued improvements and new sample preparation methods remain an important area of development. Another interesting area to explore is how data can be modeled to increase the quality of the final structures and to potentially allow the direct visualization of chemical bonding and atomic charge within crystals. Previous reports have demonstrated charge modeling for certain groups [31,82-84]. However, the extension of modeling charge for the entire protein or to visualize bonding, as has been reported for small organic molecules and materials [85,86], is still in development. Altogether, the current applications of MicroED with the ongoing technological advancements promise to make this technique an extremely useful and unique tool for structure-guided drug development.

References

1 Maveyraud, L. & Mourey, L. Protein X-ray Crystallography and Drug Discovery. *Molecules* **25**, 1030, doi:10.3390/molecules25051030 (2020).

2 Blundell, T. L. Protein crystallography and drug discovery: recollections of knowledge exchange between academia and industry. *IUCrJ* **4**, 308-321, doi:10.1107/S2052252517009241 (2017).

3 McNae, I. W. *et al.* Studying protein–ligand interactions using protein crystallography. *Crystallography Reviews* **11**, 61-71, doi:10.1080/08893110500078639 (2005).

4 Martin-Garcia, J. M. *et al.* Serial millisecond crystallography of membrane and soluble protein microcrystals using synchrotron radiation. *IUCrJ* **4**, 439-454, doi:10.1107/S205225251700570X (2017).

5 Zatsepin, N. A., Li, C., Colasurd, P. & Nannenga, B. L. The complementarity of serial femtosecond crystallography and MicroED for structure determination from microcrystals. *Current Opinion in Structural Biology*, doi:https://doi.org/10.1016/j.sbi.2019.06.004 (2019).

6 Spence, J. C. H. XFELs for structure and dynamics in biology. *IUCrJ* **4**, 322-339, doi:10.1107/S2052252517005760 (2017).
7 Shi, D., Nannenga, B. L., Iadanza, M. G. & Gonen, T. Three-dimensional electron crystallography of protein microcrystals. *Elife* **2**, e01345, doi:10.7554/eLife.01345 (2013).
8 Nannenga, B. L. & Gonen, T. The cryo-EM method microcrystal electron diffraction (MicroED). *Nature Methods* **16**, 369-379, doi:10.1038/s41592-019-0395-x (2019).
9 Egerton, R. F. Outrun radiation damage with electrons? *Advanced Structural and Chemical Imaging* **1**, 5, doi:10.1186/s40679-014-0001-3 (2015).
10 Henderson, R. The potential and limitations of neutrons, electrons and X-rays for atomic resolution microscopy of unstained biological molecules. *Q Rev Biophys* **28**, 171-193 (1995).
11 Nannenga, B. L. & Gonen, T. MicroED opens a new era for biological structure determination. *Curr Opin Struct Biol* **40**, 128-135, doi:10.1016/j.sbi.2016.09.007 (2016).
12 Jones, C. G. *et al.* The CryoEM Method MicroED as a Powerful Tool for Small Molecule Structure Determination. *ACS Central Science* **4**, 1587-1592, doi:10.1021/acscentsci.8b00760 (2018).
13 Gemmi, M. *et al.* 3D Electron Diffraction: The Nanocrystallography Revolution. *ACS Central Science*, doi:10.1021/acscentsci.9b00394 (2019).
14 Gemmi, M., La Placa, M. G. I., Galanis, A. S., Rauch, E. F. & Nicolopoulos, S. Fast electron diffraction tomography. *J Appl Crystallogr* **48**, 718-727, doi:10.1107/S1600576715004604 (2015).
15 Kolb, U., Mugnaioli, E. & Gorelik, T. E. Automated electron diffraction tomography – a new tool for nano crystal structure analysis. *Crystal Research and Technology* **46**, 542-554, doi:doi:10.1002/crat.201100036 (2011).
16 Zhang, D. L., Oleynikov, P., Hovmoller, S. & Zou, X. D. Collecting 3D electron diffraction data by the rotation method. *Zeitschrift Fur Kristallographie-Crystalline Materials* **225**, 94-102, doi:10.1524/zkri.2010.1202 (2010).
17 Boullay, P., Palatinus, L. & Barrier, N. Precession electron diffraction tomography for solving complex modulated structures: the case of Bi5Nb3O15. *Inorg Chem* **52**, 6127-6135, doi:10.1021/ic400529s (2013).
18 Jiang, J. X. *et al.* Synthesis and Structure Determination of the Hierarchical Meso-Microporous Zeolite ITQ-43. *Science* **333**, 1131-1134, doi:10.1126/science.1208652 (2011).
19 Mugnaioli, E., Gorelik, T. & Kolb, U. "Ab initio" structure solution from electron diffraction data obtained by a combination of automated diffraction tomography and precession technique. *Ultramicroscopy* **109**, 758-765, doi:10.1016/j.ultramic.2009.01.011 (2009).
20 Zhang, Y. B. *et al.* Single-Crystal Structure of a Covalent Organic Framework. *Journal of the American Chemical Society* **135**, 16336-16339, doi:10.1021/ja409033p (2013).
21 Broadhurst, E. T. *et al.* Polymorph evolution during crystal growth studied by 3D electron diffraction. *IUCrJ* **7**, 5-9, doi:10.1107/S2052252519016105 (2020).
22 Feyand, M. *et al.* Automated diffraction tomography for the structure elucidation of twinned, sub-micrometer crystals of a highly porous, catalytically active bismuth metal-

organic framework. *Angew Chem Int Ed Engl* **51**, 10373-10376, doi:10.1002/anie.201204963 (2012).
23 Nannenga, B. L., Shi, D., Hattne, J., Reyes, F. E. & Gonen, T. Structure of catalase determined by MicroED. *Elife* **3**, e03600, doi:10.7554/eLife.03600 (2014).
24 Nannenga, B. L., Shi, D., Leslie, A. G. & Gonen, T. High-resolution structure determination by continuous-rotation data collection in MicroED. *Nat Methods* **11**, 927-930, doi:10.1038/nmeth.3043 (2014).
25 de la Cruz, M. J. *et al.* Atomic-resolution structures from fragmented protein crystals with the cryoEM method MicroED. *Nat Methods* **14**, 399-402, doi:10.1038/nmeth.4178 (2017).
26 Xu, H. *et al.* Solving a new R2lox protein structure by microcrystal electron diffraction. *Science Advances* **5**, eaax4621, doi:10.1126/sciadv.aax4621 (2019).
27 Purdy, M. D. *et al.* MicroED structures of HIV-1 Gag CTD-SP1 reveal binding interactions with the maturation inhibitor bevirimat. *Proceedings of the National Academy of Sciences*, 201806806, doi:10.1073/pnas.1806806115 (2018).
28 Martynowycz, M. W., Khan, F., Hattne, J., Abramson, J. & Gonen, T. MicroED structure of lipid-embedded mammalian mitochondrial voltage-dependent anion channel. *Proceedings of the National Academy of Sciences* **117**, 32380, doi:10.1073/pnas.2020010117 (2020).
29 Liu, S. & Gonen, T. MicroED structure of the NaK ion channel reveals a Na+ partition process into the selectivity filter. *Communications Biology* **1**, 38, doi:10.1038/s42003-018-0040-8 (2018).
30 Martynowycz, M. W. *et al.* MicroED structure of the human adenosine receptor determined from a single nanocrystal in LCP. *bioRxiv*, 2020.2009.2027.316109, doi:10.1101/2020.09.27.316109 (2020).
31 Yonekura, K., Kato, K., Ogasawara, M., Tomita, M. & Toyoshima, C. Electron crystallography of ultrathin 3D protein crystals: atomic model with charges. *Proc Natl Acad Sci U S A* **112**, 3368-3373, doi:10.1073/pnas.1500724112 (2015).
32 Rodriguez, J. A. *et al.* Structure of the toxic core of alpha-synuclein from invisible crystals. *Nature*, doi:10.1038/nature15368 (2015).
33 Krotee, P. *et al.* Atomic structures of fibrillar segments of hIAPP suggest tightly mated beta-sheets are important for cytotoxicity. *Elife* **6**, doi:10.7554/eLife.19273 (2017).
34 Guenther, E. L. *et al.* Atomic-level evidence for packing and positional amyloid polymorphism by segment from TDP-43 RRM2. *Nat Struct Mol Biol* **25**, 311-319, doi:10.1038/s41594-018-0045-5 (2018).
35 Seidler, P. M. *et al.* Structure-based inhibitors of tau aggregation. *Nat Chem* **10**, 170-176, doi:10.1038/nchem.2889 (2018).
36 Warmack, R. A. *et al.* Structure of amyloid-β (20-34) with Alzheimer's-associated isomerization at Asp23 reveals a distinct protofilament interface. *Nature Communications* **10**, 3357, doi:10.1038/s41467-019-11183-z (2019).
37 van Genderen, E. *et al.* Ab initio structure determination of nanocrystals of organic pharmaceutical compounds by electron diffraction at room temperature using a Timepix quantum area direct electron detector. *Acta Crystallogr A Found Adv* **72**, 236-242, doi:10.1107/S2053273315022500 (2016).

38 Gruene, T. *et al.* Rapid Structure Determination of Microcrystalline Molecular Compounds Using Electron Diffraction. *Angew Chem Int Ed Engl* **57**, 16313-16317, doi:10.1002/anie.201811318 (2018).

39 Dick, M., Sarai, N. S., Martynowycz, M. W., Gonen, T. & Arnold, F. H. Tailoring Tryptophan Synthase TrpB for Selective Quaternary Carbon Bond Formation. *Journal of the American Chemical Society* **141**, 19817-19822, doi:10.1021/jacs.9b09864 (2019).

40 Ting, C. P. *et al.* Use of a scaffold peptide in the biosynthesis of amino acid–derived natural products. *Science* **365**, 280, doi:10.1126/science.aau6232 (2019).

41 Levine, A. M. *et al.* Crystal structure and orientation of organic semiconductor thin films by microcrystal electron diffraction and grazing-incidence wide-angle X-ray scattering. *Chemical Communications* **56**, 4204-4207, doi:10.1039/D0CC00119H (2020).

42 Brázda, P., Palatinus, L. & Babor, M. Electron diffraction determines molecular absolute configuration in a pharmaceutical nanocrystal. *Science* **364**, 667, doi:10.1126/science.aaw2560 (2019).

43 Das, P. P. *et al.* Crystal Structures of Two Important Pharmaceuticals Solved by 3D Precession Electron Diffraction Tomography. *Organic Process Research & Development* **22**, 1365-1372, doi:10.1021/acs.oprd.8b00149 (2018).

44 Banihashemi, F. *et al.* Beam-sensitive metal-organic framework structure determination by microcrystal electron diffraction. *Ultramicroscopy* **216**, 113048, doi:https://doi.org/10.1016/j.ultramic.2020.113048 (2020).

45 Vergara, S. *et al.* MicroED Structure of Au146(p-MBA)57 at Subatomic Resolution Reveals a Twinned FCC Cluster. *J Phys Chem Lett*, doi:10.1021/acs.jpclett.7b02621 (2017).

46 Simancas, J. *et al.* Ultrafast Electron Diffraction Tomography for Structure Determination of the New Zeolite ITQ-58. *Journal of the American Chemical Society* **138**, 10116-10119, doi:10.1021/jacs.6b06394 (2016).

47 Rozhdestvenskaya, I. V. *et al.* The structure of denisovite, a fibrous nanocrystalline polytypic disordered 'very complex' silicate, studied by a synergistic multi-disciplinary approach employing methods of electron crystallography and X-ray powder diffraction. *IUCrJ* **4**, 223-242, doi:10.1107/S2052252517002585 (2017).

48 Mugnaioli, E. *et al.* Ab Initio Structure Determination of Cu2–xTe Plasmonic Nanocrystals by Precession-Assisted Electron Diffraction Tomography and HAADF-STEM Imaging. *Inorganic Chemistry* **57**, 10241-10248, doi:10.1021/acs.inorgchem.8b01445 (2018).

49 Scapin, G., Potter, C. S. & Carragher, B. Cryo-EM for Small Molecules Discovery, Design, Understanding, and Application. *Cell Chemical Biology* **25**, 1318-1325, doi:https://doi.org/10.1016/j.chembiol.2018.07.006 (2018).

50 Van Drie, J. H. & Tong, L. Cryo-EM as a powerful tool for drug discovery. *Bioorganic & Medicinal Chemistry Letters* **30**, 127524, doi:https://doi.org/10.1016/j.bmcl.2020.127524 (2020).

51 Subramaniam, S., Earl, L. A., Falconieri, V., Milne, J. L. S. & Egelman, E. H. Resolution advances in cryo-EM enable application to drug discovery. *Current Opinion in Structural Biology* **41**, 194-202, doi:https://doi.org/10.1016/j.sbi.2016.07.009 (2016).

52 Clabbers, M. T. B. & Xu, H. Macromolecular crystallography using microcrystal electron diffraction. *Acta Crystallogr D Struct Biol* **77**, 313-324, doi:10.1107/S2059798320016368 (2021).
53 Clabbers, M. T. B. & Xu, H. Microcrystal electron diffraction in macromolecular and pharmaceutical structure determination. *Drug Discovery Today: Technologies*, doi:https://doi.org/10.1016/j.ddtec.2020.12.002 (2020).
54 Shi, D. *et al.* The collection of MicroED data for macromolecular crystallography. *Nat Protoc* **11**, 895-904, doi:10.1038/nprot.2016.046 (2016).
55 Nannenga, B. L. MicroED methodology and development. *Struct Dyn* **7**, 014304, doi:10.1063/1.5128226 (2020).
56 Bu, G. & Nannenga, B. L. in *CryoEM: Methods and Protocols* Vol. (In Press) *Methods in Molecular Biology* (eds B.L. Nannenga & T. Gonen) (2021).
57 Hattne, J. *et al.* MicroED data collection and processing. *Acta Crystallogr A Found Adv* **71**, 353-360, doi:10.1107/S2053273315010669 (2015).
58 Passmore, L. A. & Russo, C. J. Specimen Preparation for High-Resolution Cryo-EM. *Methods Enzymol* **579**, 51-86, doi:10.1016/bs.mie.2016.04.011 (2016).
59 Zhao, J. *et al.* A simple pressure-assisted method for cryo-EM specimen preparation. *bioRxiv*, 665448, doi:10.1101/665448 (2019).
60 Nannenga, B. L. & Gonen, T. MicroED: a versatile cryoEM method for structure determination. *Emerging Topics in Life Sciences*, doi:10.1042/etls20170082 (2018).
61 Hattne, J., Martynowycz, M. W., Penczek, P. A. & Gonen, T. MicroED with the Falcon III direct electron detector. *IUCrJ* **6**, 921-926, doi:10.1107/S2052252519010583 (2019).
62 Clabbers, M. T. B., Fisher, S. Z., Coinçon, M., Zou, X. & Xu, H. Visualizing drug binding interactions using microcrystal electron diffraction. *Communications Biology* **3**, 417, doi:10.1038/s42003-020-01155-1 (2020).
63 Xu, H. *et al.* A Rare Lysozyme Crystal Form Solved Using Highly Redundant Multiple Electron Diffraction Datasets from Micron-Sized Crystals. *Structure* **26**, 667-675 e663, doi:10.1016/j.str.2018.02.015 (2018).
64 Nederlof, I., van Genderen, E., Li, Y. W. & Abrahams, J. P. A Medipix quantum area detector allows rotation electron diffraction data collection from submicrometre three-dimensional protein crystals. *Acta Crystallogr D Biol Crystallogr* **69**, 1223-1230, doi:10.1107/S0907444913009700 (2013).
65 de la Cruz, M. J., Martynowycz, M. W., Hattne, J. & Gonen, T. MicroED data collection with SerialEM. *Ultramicroscopy* **201**, 77-80, doi:https://doi.org/10.1016/j.ultramic.2019.03.009 (2019).
66 de la Cruz, M. J. in *cryoEM: Methods and Protocols* (eds Tamir Gonen & Brent L. Nannenga) 321-327 (Springer US, 2021).
67 Hattne, J. *et al.* Analysis of Global and Site-Specific Radiation Damage in Cryo-EM. *Structure* **26**, 759-766 e754, doi:10.1016/j.str.2018.03.021 (2018).
68 Hattne, J. Low-Dose Data Collection and Radiation Damage in MicroED. *Methods Mol Biol* **2215**, 309-319, doi:10.1007/978-1-0716-0966-8_15 (2021).
69 Battye, T. G., Kontogiannis, L., Johnson, O., Powell, H. R. & Leslie, A. G. iMOSFLM: a new graphical interface for diffraction-image processing with MOSFLM. *Acta Crystallogr D Biol Crystallogr* **67**, 271-281, doi:10.1107/S0907444910048675 (2011).

70 Leslie, A. G. W. & Powell, H. R. Processing diffraction data with mosflm. **245**, 41-51, doi:10.1007/978-1-4020-6316-9_4 (2007).
71 Kabsch, W. Xds. *Acta Crystallogr D Biol Crystallogr* **66**, 125-132, doi:10.1107/S0907444909047337 (2010).
72 Clabbers, M. T. B., Gruene, T., Parkhurst, J. M., Abrahams, J. P. & Waterman, D. G. Electron diffraction data processing with DIALS. *Acta Crystallogr D Struct Biol* **74**, 506-518, doi:10.1107/S2059798318007726 (2018).
73 Martynowycz, M. W. & Gonen, T. Ligand Incorporation into Protein Microcrystals for MicroED by On-Grid Soaking. *Structure* **29**, 88-95.e82, doi:https://doi.org/10.1016/j.str.2020.09.003 (2021).
74 Sippel, K. H. *et al.* High-resolution structure of human carbonic anhydrase II complexed with acetazolamide reveals insights into inhibitor drug design. *Acta Crystallogr Sect F Struct Biol Cryst Commun* **65**, 992-995, doi:10.1107/s1744309109036665 (2009).
75 Martynowycz, M. W., Zhao, W., Hattne, J., Jensen, G. J. & Gonen, T. Collection of Continuous Rotation MicroED Data from Ion Beam-Milled Crystals of Any Size. *Structure* **27**, 545-548.e542, doi:https://doi.org/10.1016/j.str.2018.12.003 (2019).
76 Duyvesteyn, H. M. E. *et al.* Machining protein microcrystals for structure determination by electron diffraction. *Proc Natl Acad Sci U S A* **115**, 9569-9573, doi:10.1073/pnas.1809978115 (2018).
77 Li, X., Zhang, S., Zhang, J. & Sun, F. In situ protein micro-crystal fabrication by cryo-FIB for electron diffraction. *Biophysics reports* **4**, 339-347, doi:10.1007/s41048-018-0075-x (2018).
78 Polovinkin, V. *et al.* Demonstration of electron diffraction from membrane protein crystals grown in a lipidic mesophase after lamella preparation by focused ion beam milling at cryogenic temperatures. *J Appl Crystallogr* **53**, 1416-1424, doi:10.1107/S1600576720013096 (2020).
79 Zhu, L. *et al.* Structure Determination from Lipidic Cubic Phase Embedded Microcrystals by MicroED. *Structure* **28**, 1149-1159.e1144, doi:https://doi.org/10.1016/j.str.2020.07.006 (2020).
80 Bücker, R. *et al.* Serial protein crystallography in an electron microscope. *Nature Communications* **11**, 996, doi:10.1038/s41467-020-14793-0 (2020).
81 Wang, B., Zou, X. & Smeets, S. Automated serial rotation electron diffraction combined with cluster analysis: an efficient multi-crystal workflow for structure determination. *IUCrJ* **6**, 854-867, doi:10.1107/S2052252519007681 (2019).
82 Yonekura, K. *et al.* Ionic scattering factors of atoms that compose biological molecules. *IUCrJ* **5**, 348-353, doi:doi:10.1107/S2052252518005237 (2018).
83 Yonekura, K. & Maki-Yonekura, S. Refinement of cryo-EM structures using scattering factors of charged atoms. *J Appl Crystallogr* **49**, doi:10.1107/s1600576716011274 (2016).
84 Blum, T. B. *et al.* Statistically correcting dynamical electron scattering improves the refinement of protein nanocrystals, including charge refinement of coordinated metals. *Acta Crystallogr D Struct Biol* **77**, 75-85, doi:10.1107/S2059798320014540 (2021).

85 Wu, J. S. & Spence, J. C. Structure and bonding in alpha-copper phthalocyanine by electron diffraction. *Acta Crystallogr A* **59**, 495-505, doi:10.1107/S0108767303016866 (2003).
86 Zuo, J. M., Kim, M., O'Keeffe, M. & Spence, J. C. H. Direct observation of d-orbital holes and Cu-Cu bonding in Cu2O. *Nature* **401**, 49-52, doi:Doi 10.1038/43403 (1999).

Acknowledgements

The Nannenga lab is supported by the National Institutes of Health R01GM124152 and R21GM135784 and the National Science Foundation DMR-1942084. The Gonen lab is supported by the National Institutes of Health P41GM136508 and by funds from the Howard Hughes Medical Institute.

Author contributions

The authors contributed equally to all aspects of the article.

Competing interests

The authors declare no competing interests.

Table of Contents blurb

The structure of ligand protein complexes are critical for understanding protein fuction and drug design efforts. This review discusses the use and future prospects of the microcrystal electron diffraction (MicroED) method for determining the structure of protein-ligand complexes from crystals too small for other methods.

Summary

Microcrystal electron diffraction (MicroED) can determine the structure of proteins from crystals orders of magnitude smaller than other methods. Here the application of MicroED to protein-ligand complexes is reviewed.

Figures

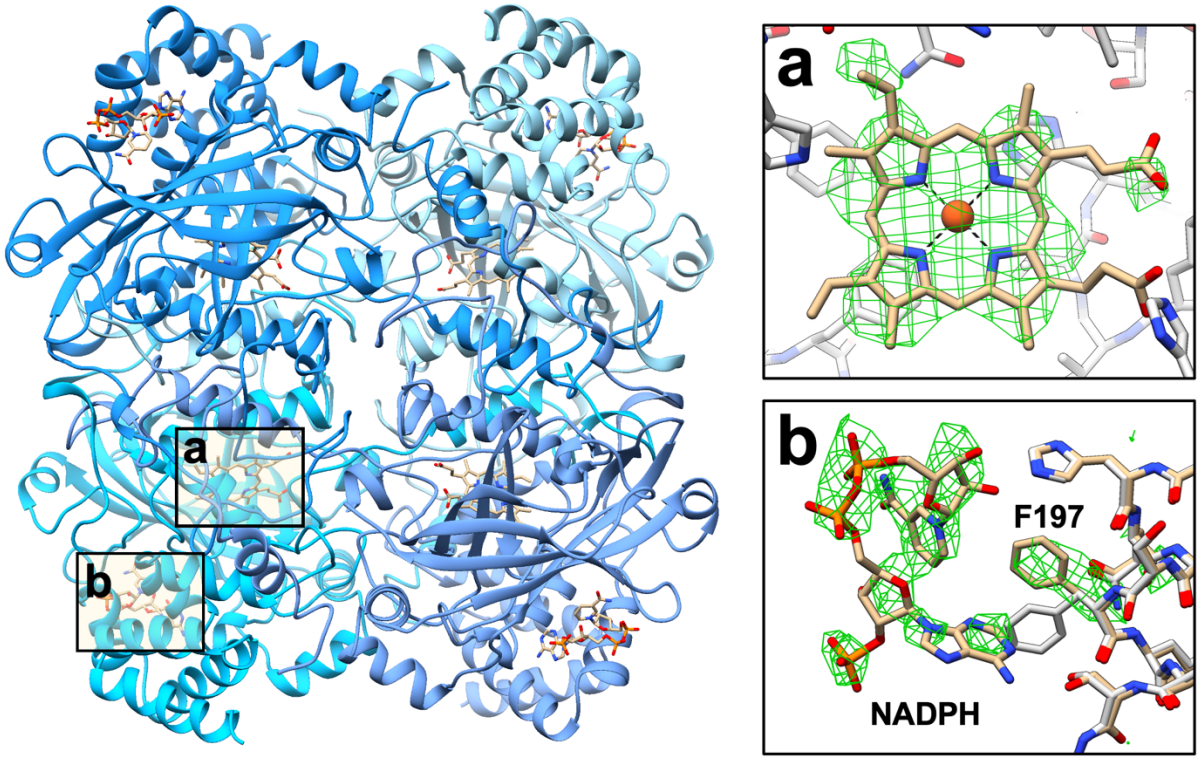

Fig. 1 | **MicroED structure of catalase with bound heme and NADPH. a** | Because the heme ligands are present in the catalase protein, when they are omitted from the model, clear positive signal in the difference maps (F_{obs} - F_{calc}) can be seen (green density), validating that these ligands are present in the structure and allowing the modeling of the bound heme within the structure. **b** | When maps are calculated using a model without bound NADPH (grey model), the difference map shows positive potential (green density) for the NADPH as well as the correct position for phenylalanine 197 (tan model). Models are from Ref. 23 (PDB ID: 3j7b)

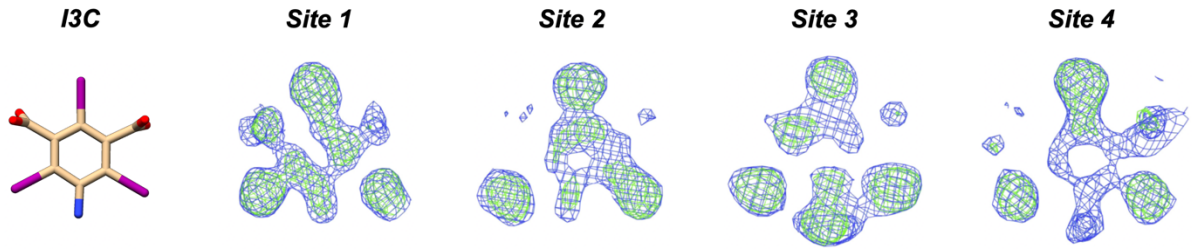

Fig. 2. 5-amino-2,4,6-triodoisophthalic acid (I3C) sites in Proteinase K. The structure of I3C and the resulting MicroED density maps of the four I3C sites in Proteinase K are shown. The density maps, which are the result of the MicroED experiment and used for model building, are shown as both $2F_{obs}$ - F_{calc} (blue) and positive F_{obs} - F_{calc} (green) difference maps. These four sites all refined to an occupancy of 75%, 58%, 61% and 59% for sites 1 to 4, respectively. These occupancies are higher for MicroED when compared to the X-ray structure, which were reported to be 75%, 21%, 0%, and 12%, for sites 1 to 4, respectively[73]. Models are from Ref. 73 (PDB ID: 7jsy)

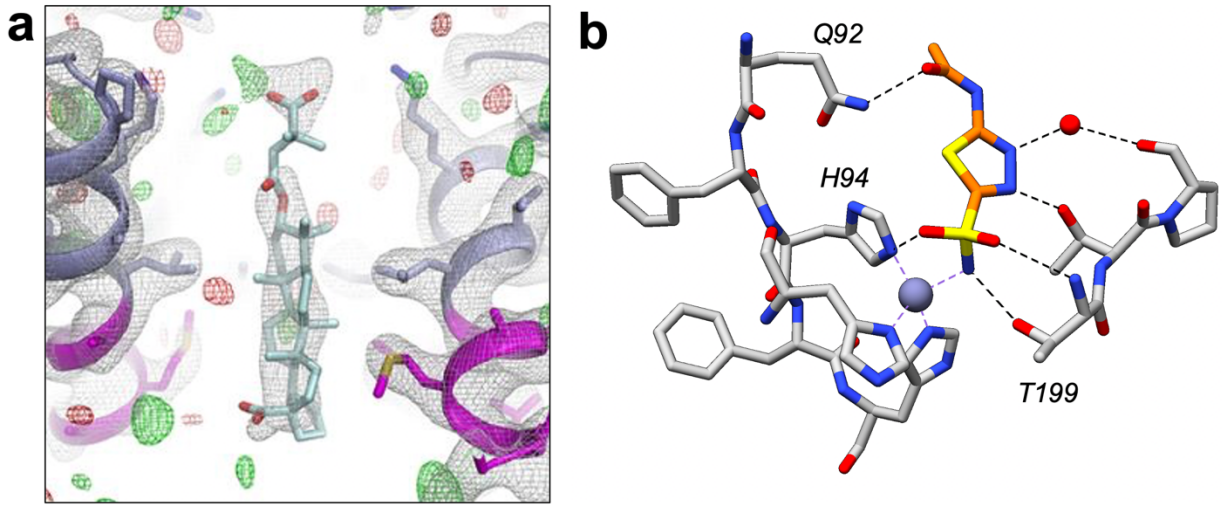

Fig. 3. MicroED facilitates the modeling of inhibitors within the protein structure. **a** | Modelled orientation of bevirimat bound to HIV-1 Gag. Here, the up orientation of bevirimat is depicted. **b** | Modeled human carbonic anhydrase (HCA II)-acetazolamide (AZM) interactions with the and three highlighted amino acids and the Zn^{2+} metal cofactor. Carbon, nitrogen, oxygen, and sulfur atoms are colored in gray, blue, red, and yellow, respectively and the Zn^{2+} metal cofactor is shown as a dark-gray sphere. In each case, the structure determined by MicroED was able to allow the modeling of each bound inhibitor within the structure, which shows the key interactions between the molecule and the protein.

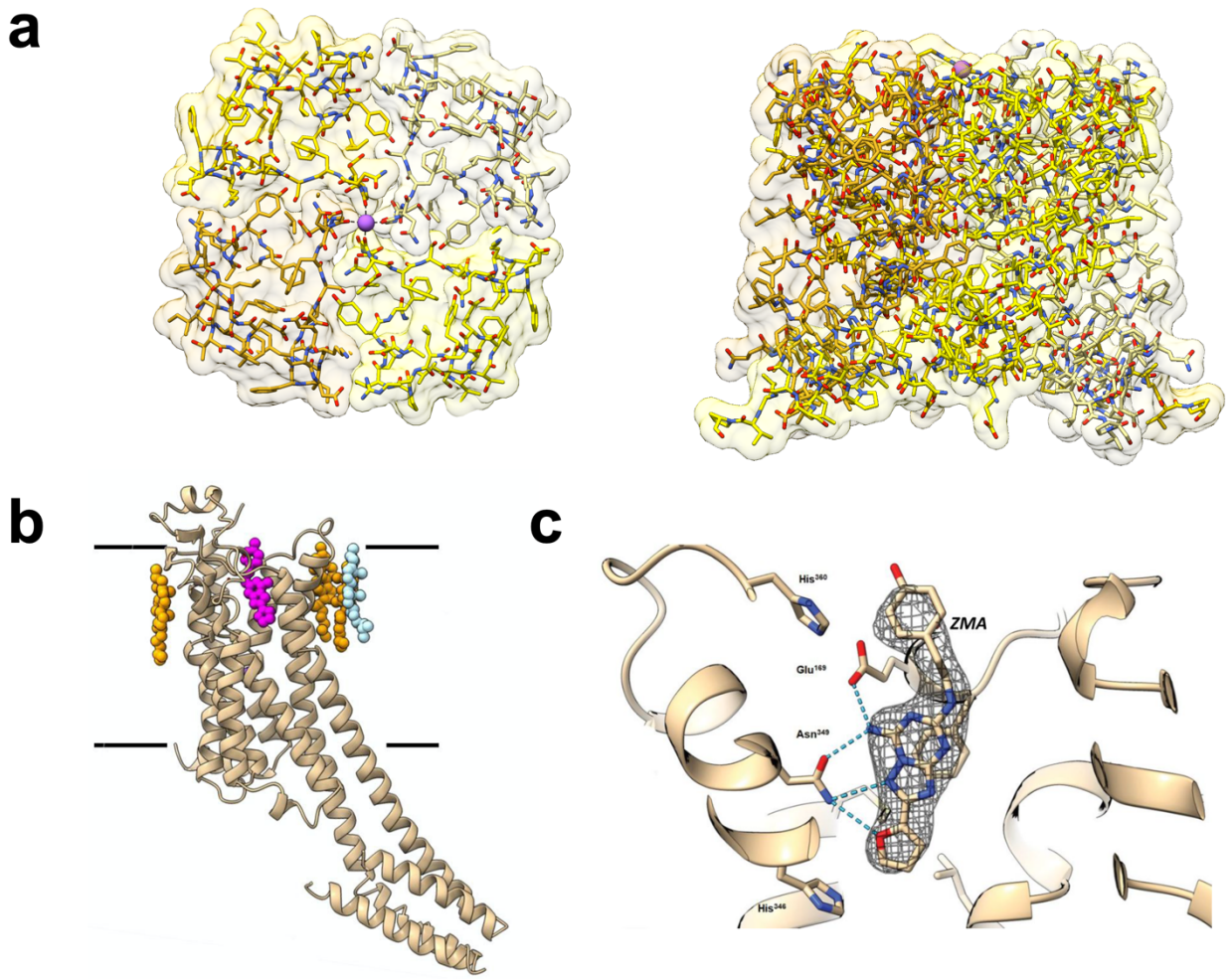

Fig. 4. **Membrane protein structures determined by MicroED. a** | NaK was the first membrane protein structure determined by MicroED and allowed the modeling of water molecules and sodium ions within the channel pore. The model and surface view of NaK is shown from the top (left) and side (right) relative to the membrane. The models shown in a are from Ref 29 (PDB 6cpv). **b** | The structure of the human adenosine A_{2A} receptor, the first G-protein coupled receptors (GPCR) structure determined by MicroED, viewed from the side. The membrane bilayer is indicated by the black lines. The antagonist ligand (ZMA) is shown in pink and cholesterol is shown in orange (known positions) and blue (newly determined position). **c** | A magnification of the binding pocking in b where the MicroED determined structure shows clear density for the co-crystallized ZMA antagonist bound to the receptor. The models shown for b and c are from Ref. 30 (PDB ID: 7rm5)